Characterizing the Achievable Throughput in Wireless Networks with Two Active RF chains

Yang Yang*, Bo Chen†, Kannan Srinivasan†, Ness B. Shroff*†
*Department of Electrical and Computer Engineering, The Ohio State University, Columbus 43210, OH
†Department of Computer Science and Engineering, The Ohio State University, Columbus 43210, OH

***Abstract*—Recent breakthroughs in wireless communication show that by using new signal processing techniques, a wireless node is capable of transmitting and receiving simultaneously on the same frequency band by activating both of its RF chains, thus achieving full-duplex communication and potentially doubling the link throughput. However, with two sets of RF chains, one can build a half-duplex multi-input and multi-output (MIMO) system that achieves the same gain. While this gain is the same between a pair of nodes, the gains are unclear when multiple nodes are involved, as in a general network. The key reason is that MIMO and full-duplex have different interference patterns. A MIMO transmission blocks transmissions around its receiver and receptions around its transmitter. A full-duplex bidirectional transmission blocks any transmission around the two communicating nodes, but allows a reception on one RF chain. Thus, in a general network, the requirements for the two technologies could result in potentially different achievable throughput regions.**

This work investigates the achievable throughput performance of MIMO, full-duplex and their variants that allow simultaneous activation of two RF chains. It is the first work of its kind to precisely characterize the conditions under which these technologies outperform each other for a general network topology under a binary interference model. The analytical results in this paper are validated using software-defined radios.

I. Introduction

The key challenge faced by current wireless communication systems is to provide wireless access with high data-rates. Multi-antenna/Multi-RF chain techniques serve as an important means to improve spectrum efficiency [1]. It has been long known that by using multiple RF chains at both the transmitter and the receiver, and transmitting independent data streams on different antennas, MIMO can increase the spectral efficiency by a factor of the number of active RF chains.

Recent developments in wireless full-duplex technology introduce another way to utilize multiple active RF chains. It has been shown that while one RF chain is used for transmission, another one can be simultaneously used for reception. This is enabled by using advanced signal processing techniques between the transmit RF chain and receive RF chain to reduce self interference [2]–[4]. Since the interference from the transmitting antenna is cancelled at the receiving antenna, a twofold gain in throughput can be realized for a bidirectional flow, which is the same gain as that can be achieved by 2×2 MIMO multiplexing for a unidirectional flow.

It should be noted that different multi-RF chain techniques require different hardware configurations. When there are at least two antennas and two active RF chains, a node can have three different transceiver structures as shown in Fig. 1: (b) For a node to operate in full-duplex mode, it needs to have a complete set of RF chains plus a cancellation module which cancels self-interference [2]–[4]; (c) MIMO mode can be enabled when there are two complete sets of RF chains; (d) If a node has two complete sets of RF chains plus a self-interference cancellation module, then it can operate in either MIMO or full-duplex communication. The SISO mode shown in Fig. 1(a) is here just for reference.

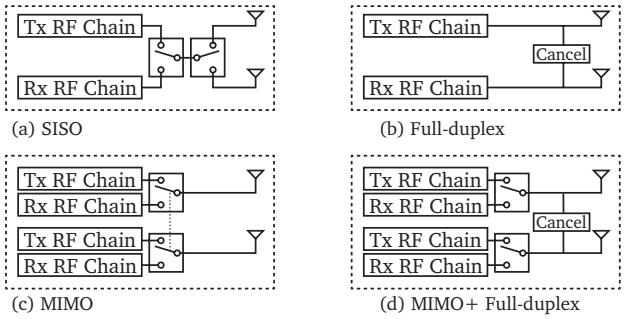

Fig. 1. Block diagram of transceiver structures with two antennas for (a) SISO half-duplex, (b) full-duplex, (c) MIMO, and (d) MIMO plus full-duplex. If a node has the transceiver structure shown in (d), then it can enable either MIMO or full-duplex communication. In transceiver structures (b) and (d), for ease of exposition, the full-duplex cancellation circuit is drawn in analog RF end, but the cancellation can also happen in analog baseband and digital domain.

This raises a natural question: under what conditions might a wireless system get more throughput gain from one technique over the other? While it is easy to compare the throughput gain of MIMO multiplexing and full-duplex in an elementary setting such as a link between a pair of nodes, when we view it form a general wireless network's perspective, the answer is less clear. In this work, we mainly focus on transceiver structures shown in Fig. 1(b) (c) and (d), while the SISO mode in Fig. 1(a) is just for comparison purposes.

Characterizing the throughput region of a general wireless network has been an open problem for a long time, partially because the intrinsic broadcast nature of wire-

978-14799-3360-0/14/$31.00 ©2014 IEEE

less communication leads to a very complex interference coupling among simultaneous transmissions. The de facto method to manage interference coupling and coordinate wireless transmissions is to treat interference simply as noise and to avoid it by scheduling links that do not cause serious interference with each other. Generally speaking, under scheduling, a group of wireless links can be activated at the same time only when they all satisfy their SINR constraints. Recent developments in physical layer wireless technologies show that by dealing with interference in a smart way rather than simply treating it as noise and avoiding it, e.g., by using the *interference alignment* technique [5], or *noisy network coding* [6], a higher network throughput can be obtained versus traditional interference avoidance techniques. However, almost all of these techniques require extensive knowledge of the entire network state information, and it is still an open problem regarding how to incorporate them into the scheduling problem under a general wireless network.

Therefore, in this work, we restrict our focus to the case when *interference in the wireless network is treated as noise* and *the channel state information is known only at the receiver*, and leave the accommodation of more advanced physical layer techniques such as interference alignment [5] as future work. To characterize the interference relationship between the nodes, we assume a binary interference channel, where any two nodes in a wireless network either interfere with each other, or do not interfere at all. At any scheduled time-slot, the rate of a link is simply represented by the number of data streams that are transmitted on that link, which means that the rate of a link is either 0, 1, or 2. Henceforth, whenever we refer to the optimal throughput region or the achievable throughput it is with respect to this interference model.

It should be noted that even with this simplified 0-1 interference model and simplified throughput definition, the comparison of the throughput regions achieved by different multi-RF chain techniques is a challenging task. The fundamental reason is that different transmission modes leave different *interference footprints* on the rest of the network. Consider a simple scenario shown in Fig. 2. Assume that node A and node B lie in a wireless network where every node has two set of RF chains and can operate in either MIMO or full-duplex mode, and the circle around these two nodes indicates their interference regions. If there is a bidirectional transmission between node A and node B, as shown in Fig. 2(a), then any node within their interference region cannot be transmitting, since both nodes A and B are utilizing both of their two RF chains and no extra interference can be decoupled using multiple receive RF chains. At the same time, if a node lies in and only in one of node A and node B's interference region, then it cannot be receiving more than one data stream, because its two RF chains can at most resolve two spatially multiplexed streams, one of which is the interference from either node A or node B. On the other hand, when node A is transmitting two spatially multiplexed data streams to node B, as shown in Fig. 2(b), then it is easy to see that any node within A's interference region cannot be receiving any number of data streams, because every node has only two RF chains and, therefore, cannot decode more than two spatially multiplexed streams. For the same reason, any node within B's interference region cannot be transmitting any number of data streams.

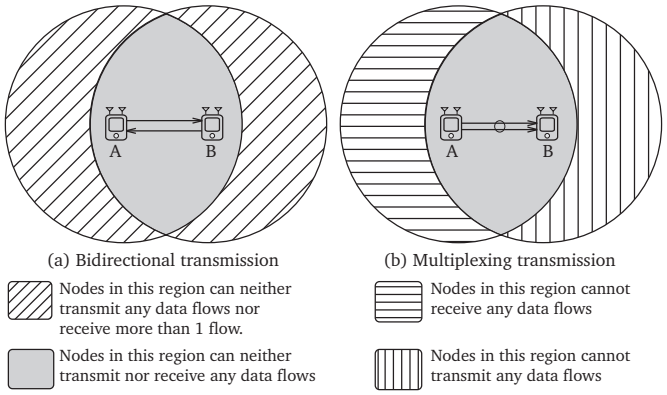

Fig. 2. The interference footprint of the transmission between node A and node B in a wireless network where each node has two active RF chains and can enable either full-duplex or MIMO transmission. The circle around node A/B indicates its interference range. In (a), both node A and node B are operating in full-duplex, and a bidirectional transmission is established between the two nodes; in (b), two spatially multiplexed streams are sent from node A to node B.

The intellectual merit of this paper lies in answering the following two key questions:

1) In a general wireless network with at least two antennas and at most two active RF chains at every node, for any two different RF hardware structures, what is the relationship between their achievable throughput regions?
2) For any two different RF hardware configurations, under what *exact* network scenario can one achieve a strictly larger throughput region than the other?

Given that there are four different RF hardware configurations as shown in Fig. 1, the above two questions can be broken down into several smaller questions, such as: Is there a network scenario under which full-duplex can achieve a better throughput region than MIMO? Does MIMO alone achieve all the throughput gains brought by full-duplex in any scenario? When MIMO and full-duplex coexist in a network, can we achieve a better throughput region than MIMO or full-duplex alone? If so, under what network scenario? The rest of this paper answers these questions and provides a very clear guideline on which network topologies and traffic patterns could result in improvement for one technology over another.

II. System Model

We consider a wireless network where each wireless node has two sets of RF chains and there is no channel

state information at the transmitter. We assume a binary symmetric interference structure between wireless nodes, where the transmission of a node either interferes with the reception of another node, or does not interfere at all, and when node A interferes with node B, node B also interferes with node A. Note that this binary interference model is widely adopted in the scheduling literature [7]–[10], and serves as an important first step towards scheduling under the more complex, SINR interference model [11], [12].

Let $\mathcal{G} = \{\mathcal{N}, \mathcal{E}\}$ denote the undirected network topology graph, which captures the interference relationship between the wireless nodes. Here $\mathcal{N}$ is the set of wireless nodes, and $\mathcal{E}$ is the set of edges between the wireless nodes. For $A, B \in \mathcal{N}$, $\{A, B\} \in \mathcal{E}$ if and only if A and B interfere with each other. Among these edges, we further denote $\mathcal{E}_L$ as the set of edges where a direct wireless data-link can be established between the two end nodes. Then the set of data links can be denoted as

$$\mathcal{L} = \{(A, B), (B, A) | \{A, B\} \in \mathcal{E}_L\}.$$

Since every node has two antennas, for each data link, there can either be one data stream, or a pair of multiplexed data streams, enabled by MIMO multiplexing. Therefore, we further denote the set of all possible data streams as

$$\mathcal{L}_{12} = \left\{(A, B)^1, (A, B)^2 | (A, B) \in \mathcal{L}\right\},$$

where $(A, B)^1$ stands for a single data stream from node A to node B, and $(A, B)^2$ stands for two multiplexed data streams from node A to node B. In the rest of the paper we make a simplified assumption that $\mathcal{E}_L = \mathcal{E}$. However, our analysis can be readily extended to the case when $\mathcal{E}_L \subset \mathcal{E}$ [13].

A. Constraint set

As described in the Introduction, when a node has at least two antennas and can simultaneously activate two RF chains, it can have at least three different transceiver structures as shown in Fig. 1. Given our assumption that the channel state information is known only at the receiver, it is easy to see that a wireless node has the potential to operate in either one of the ten modes shown in Fig. 3. Among these ten modes, mode 1 and 2 are SISO modes, mode 3 and 4 are full-duplex modes, mode 5 and 6 are MIMO multiplexing modes, and mode 7 through 10 are multi-user MIMO modes.

As we have discussed in the introduction, which modes can be activated (or not) depends on the node's hardware configuration. Given that there are four RF architectures, as shown in Fig. 1, we can set up the following four constraint sets which restrict the modes a node can operate in, based on its RF configuration.

1) Single-input Single-output (SS) constraint set: In this constraint set, each node has only one set of RF chains with no cancellation module, as shown in Fig. 1(a). As a result, each node can only operate in SISO modes, which are mode 1 and mode 2 in Fig. 3. Note that this constraint set does not allow the simultaneous activation of two RF chains, and it serves only as a baseline for showing the throughput gains of two active RF chains.

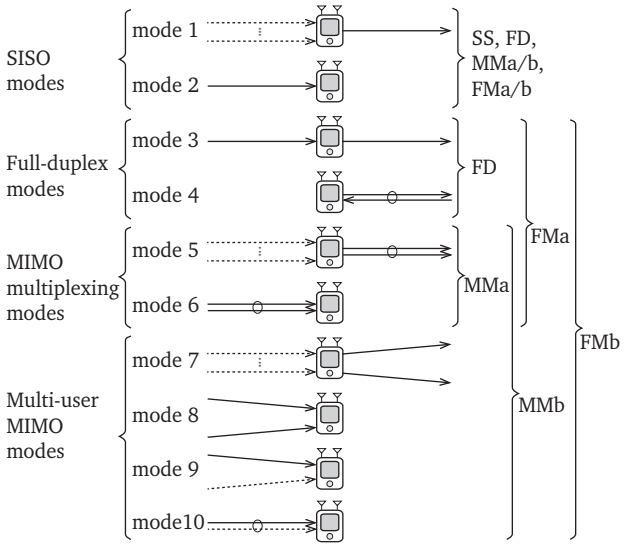

Fig. 3. Different communication modes. A dashed arrow represents an interference flow. A circle on two flows indicates that the two flows are transmitted by the same transmitter node. In Single-input Single-output (SISO) modes, a user can either receive a single flow (mode 2), or transmit a single flow while withstanding any number of interference flows (mode 1); in full-duplex modes, a user can transmit one flow and receive another flow simultaneously (mode 3 and mode 4); in MIMO multiplexing modes, a user can transmit/receive two independent flows to/from another user (mode 5/mode 6); in multi-user MIMO mode, a user can transmit/receive two flows to/from two different users (mode 7/mode 8), or receive one flow while withstanding another interference flow (mode 9 and mode 10).

2) Full-duplex (FD) constraint set: Nodes in this constraint set have one complete set of RF chains plus a cancellation module, as shown in Fig. 1(b), where one antenna is designated as a transmit antenna and the other as a receive antenna. The cancellation module cancels the self-interference from the transmit antenna to the receive antenna [2]–[4]. Therefore, the node can operate in both SISO and full-duplex modes, which are modes 1-4 in Fig. 3

3) MIMO (MM) constraint set: In this set, each node has two complete sets of RF chains, as shown in Fig. 1. Hence, it can operate in MIMO communication modes, meaning that a node can either transmit or receive two data streams simultaneously. In Fig. 3, modes 5-10 form MIMO modes, where modes 5 and 6 correspond to MIMO multiplexing, and modes 7-10 represent multi-user MIMO. In order to differentiate between MIMO multiplexing and multi-user MIMO, we define two sub-constraint-sets, namely **MMa** and **MMb** constraint sets. In the MMa set, multi-user MIMO is not allowed and all the nodes can operate in one of modes 1, 2, 5, and 6. In MMb set, both MIMO multiplexing and multi-user MIMO are allowed, meaning that all the nodes can operate in one of modes

1, 2, and 5-10.

4) Full-duplex MIMO (FM) constraint set: In this set, each node has two complete sets of RF chains and a cancellation module, which serves as the self-interference cancellation circuit. Nodes in this mode can operate in either full-duplex modes or MIMO modes. Similarly, as in the previous constraint set, to differentiate between MIMO multiplexing and multi-user MIMO, we define two sub-constraint-sets, namely **FMa** and **FMb** set. In the FMa set, nodes can operate in either one of mode 1 to mode 6, while in FMb set, nodes can operate in any of the ten modes shown in Fig. 3.

A subset of data links $S \subseteq \mathcal{L}_{12}$ is called a *feasible activation set* under a constraint set if the links within that subset can be activated at the same time without violating the modes of transmission defined by that constraint set. We denote the set of all feasible activation sets under a certain constraint set as $\mathbb{S}_{\text{Constr}}(\mathcal{G})$. For example,

$$\mathbb{S}_{\text{SS}}(\mathcal{G}) = \big\{S \subseteq \mathcal{L}_{12} | S \text{ is a feasible activation set in topology } \mathcal{G} \text{ under SS constraint set}\big\}.$$

We also call $S \in \mathbb{S}_{\text{SS}}(\mathcal{G})$ an SS-feasbile schedule. We use a vector in $\{0,1,2\}^{|\mathcal{L}|}$ to denote a schedule S such that the k^{th} element is set to 1 if a single data stream is scheduled on link $k \in \mathcal{L}$, set to 2 if two multiplexed streams are scheduled on link $k \in \mathcal{L}$, and set to 0 otherwise. We denote the vector representing schedule S as $\vec{R}(S)$, then it is formally defined as follows:

$$\vec{R}(S) = \big[R_{(A,B)}(S), (A,B) \in \mathcal{L}\big], \text{ and}$$
$$R_{(A,B)}(S) = \begin{cases} 1 & \text{if } (A,B)^1 \in S \\ 2 & \text{if } (A,B)^2 \in S \\ 0 & \text{otherwise} \end{cases}. \quad (1)$$

$\vec{R}(S)$ counts the number of independent data streams that are packed into schedule S, hence we also call it the rate vector of schedule S.

Given the set of all activation sets $\mathbb{S}_{\text{Constr}}(\mathcal{G})$, we denote the set of all corresponding rate vectors as $\mathbb{R}_{\text{Constr}}(\mathcal{G}) = \big\{\vec{R}(S) | S \in \mathbb{S}_{\text{Constr}}(\mathcal{G})\big\}$, and let $\text{Co}(\mathbb{R}_{\text{Constr}}(\mathcal{G}))$ denote its convex hull, where the convex hull $\text{Co}(A)$ of a set A is defined as

$$\text{Co}(A) \triangleq \left\{ \sum_i w_i \vec{\alpha}_i \Big| w_i \geq 0, \sum w_i = 1, \vec{\alpha} \in A \right\}.$$

The *throughput region* under a given scheduling policy is defined as the set of vectors $\vec{\lambda} = \{\lambda_1, \lambda_2, \ldots, \lambda_{|\mathcal{L}|}\}$ for which the long term average throughput achieved over link i can be greater than or equal to λ_i for every i. In this sense, the *optimal throughput region* that can be achieved by scheduling is known to be [14]

$$\mathbb{D}_{\text{Constr}}(\mathcal{G}) = \left\{ \vec{\lambda} | \vec{\lambda} \preccurlyeq \vec{\theta}, \text{ for some } \vec{\theta} \in \text{Co}(\mathbb{R}_{\text{Constr}}(\mathcal{G})) \right\},$$

which also equals to $\text{Co}\{\mathbb{R}_{\text{Constr}}(\mathcal{G}), \vec{0}\}$. A summary of all the notations can be found in Table I. *Without causing confusion, in the rest of the paper, we will abuse notation slightly by writing $\mathbb{S}_{Constr}(\mathcal{G})$, $\mathbb{R}_{Constr}(\mathcal{G})$ and $\mathbb{D}_{Constr}(\mathcal{G})$ as $\mathbb{S}_{Constr}$, $\mathbb{R}_{Constr}$, and $\mathbb{D}_{Constr}$, respectively.*

TABLE I
NOTATIONS (network graph $\mathcal{G}$ with SS constraint set)

Notation	Description
$\mathcal{L}_{12}$	The set of all data streams (include single stream and multiplexed stream) in $\mathcal{G}$.
$S \subset \mathcal{L}_{12}$	A subset of data streams, also called an activation set, or a schedule.
$\vec{R}(S)$	The rate vector of schedule S defined in Equation (1).
$\mathbb{S}_{\text{SS}}(\mathcal{G})$	The set of all feasible schedules under SS constraint set.
$\mathbb{R}_{\text{SS}}(\mathcal{G})$	The set of rate vectors of all the schedules in $\mathbb{S}_{\text{SS}}(\mathcal{G})$.
$\mathbb{D}_{\text{SS}}(\mathcal{G})$	The optimal throughput region of $\mathcal{G}$ under SS constraint set.

III. OPTIMAL THROUGHPUT REGION

Given the six constraint sets and the definition of the optimal throughput region that can be achieved by scheduling, a natural question to ask is what relationship exists between the achievable throughput regions under different constraint sets. In other words, does an upgrade in the RF hardware bring additional throughput gain in the wireless network when scheduling is used? If the throughput region achieved by constraint set A is not always the same as that achieved by constraint set B for any wireless network, under what network condition can one of constraint sets A and B provide a strictly better throughput region than the other? This section answers these questions.

While it is easy to compare the throughput achieved by different constraint sets under an elementary wireless network, when we consider a more general wireless network, it is not clear if some modes in Fig. 3 are always better than some others, because different modes of transmission of a node leave different interference footprints on the rest of the network, as discussed in the introduction.

The theorem below characterizes the relationship between the throughput regions that are achieved by the six constraint sets for any network graph.

Theorem 1. *For any network topology graph $\mathcal{G}$, the throughput regions under SS, FD, MMa/MMb, and FMa/FMb constraint set have the following relationship:*

$$\mathbb{D}_{MMa} = 2\mathbb{D}_{SS} \quad (2)$$
$$\mathbb{D}_{SS} \overset{(a)}{\subseteq} \mathbb{D}_{FD} \overset{(b)}{\subseteq} \mathbb{D}_{MMa} \overset{(c)}{=} \mathbb{D}_{FMa} \overset{(d)}{\subseteq} \mathbb{D}_{MMb} \overset{(e)}{\subseteq} \mathbb{D}_{FMb} \quad (3)$$

Remark 1.1. Equation (2) is obvious because by using 2 by 2 MIMO multiplexing allowed in MMa constraint set, each link in a SS-feasible schedule can transmit two independent data streams simultaneously instead of one, and therefore achieving twice the throughput. Part (a), (d), and (e) in Equation (3) are also straightforward, since

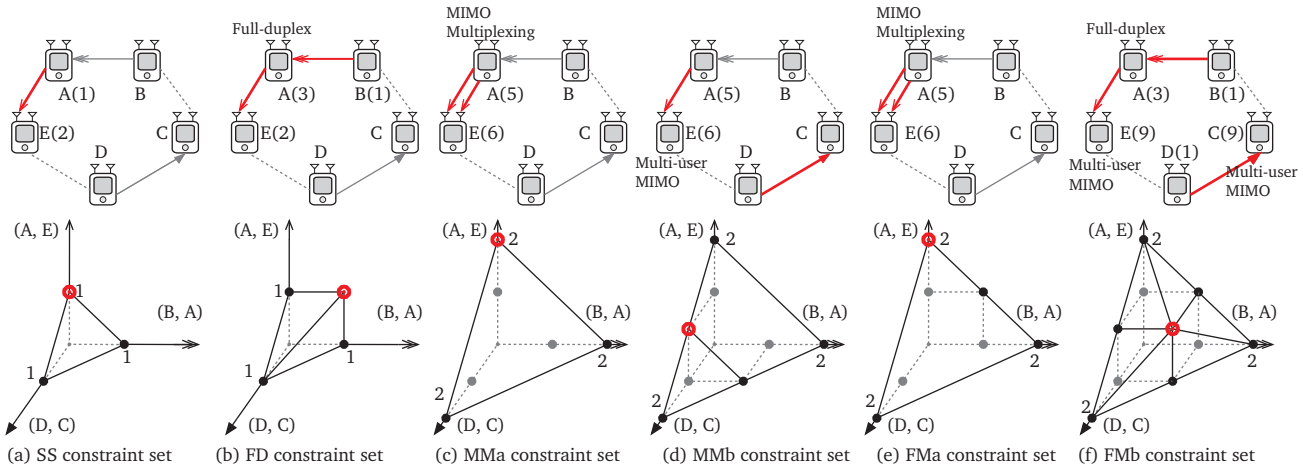

(a) SS constraint set (b) FD constraint set (c) MMa constraint set (d) MMb constraint set (e) FMa constraint set (f) FMb constraint set

Fig. 4. Throughput regions of a five-node cyclic network under SS, FD, MMa/MMb, and FMa/FMb constraint sets. Here we only focus on the data links from A to E, from D to C and from B to A. Each dot in the throughput region plot represents a feasible schedule under the corresponding constraint set. The red arrows on each network graph illustrate one such feasible schedule, while the parentheses after each node represents its communication mode, and these feasible schedules correspond to the big red dots on the throughput region plot. (a) When every node has only one active RF chain at any time, no more than one data stream in these three links can be simultaneously activated. (b) When every node has full-duplex capability, then a data stream from B to A and a data stream from A to E can be activated together. (c,d,e) Under MMa/MMb/FMa constraint set, at any time we cannot support more than 2 simultaneous data streams in the three links. (f) When every node have both multi-user MIMO and full-duplex capabilities, three data streams, one for each data link, can be activated together. The comparison between (b,d) and (f) shows that a strictly larger throughput region can be achieved when each node can choose to operate in either MIMO or full-duplex mode, than the case when only MIMO, or only full-duplex is supported.

the available modes under SS, MMa, and MMb constraint set are included in FD, MMb, and FMb constraint set, respectively.

Remark 1.2. Part (b) in Equation (3) says that if the two antennas on each node can only be used to enable full-duplex transmission, i.e., each node has the RF structure of Fig. 1(b), then the achievable throughput region, for any network graph, is always a subset of that achieved in the case when each node can operate in MIMO multiplexing modes, enabled by two complete sets of RF chains. Part (c) implies that, when multi-user MIMO is not allowed, then upgrading the RF hardware from that in Fig. 1(c) to that in Fig. 1(d) does not increase the achievable throughput region, for any network graph. Fig. 4 gives an illustration of the relationship between the different throughput regions in a five-node cyclic network graph.

Remark 1.3. In general, establishing the relationship of these throughput regions for a network on case by case basis seems very hard because it depends on network topologies and traffic patterns. However, by creating the notion of the 10 modes, in the proof, we are able to circumvent this inherent difficulty and decouple the problem from a network back to what happens at the end nodes of a link belonging to each activation set.

Proof: We focus on the proof of parts (b) and (c) in Equation (3). Since the available modes in FD constraint set is a subset of that in FMa constraint set, for every $S_1 \in \mathbb{S}_{\text{FD}}$, $S_1 \in \mathbb{S}_{\text{FMa}}$. Therefore, to prove $\mathbb{D}_{\text{FD}} \subseteq \mathbb{D}_{\text{MMa}} = \mathbb{D}_{\text{FMa}}$, it suffices to show that for every $S_1 \in \mathbb{S}_{\text{FMa}}$, we can construct $S_2, S_3 \in \mathbb{S}_{\text{MMa}}$ such that $2\vec{R}(S_1) = \vec{R}(S_2) + \vec{R}(S_3)$.

Let us start with an activation set $S_1 \in \mathbb{S}_{\text{FMa}}$. From the definition of the FMa constraint set, we know that each link in S_1 must fall into one of the following four categories based on the operation modes of its two end nodes. (i) The transmitter is in mode 1 and the receiver is in mode 2. (ii) Both the transmitter and the receiver are in mode 4. (iii) Either the transmitter or the receiver is in mode 3. (iv) The transmitter is in mode 5 and the receiver is in mode 6.

Then, let us construct two activation sets S_2 and S_3 based on S_1 by going through links in all these four different categories. Initially set both S_2 and S_3 as the empty set.

(i). If link $(A,B)^1 \in S_1$ falls into the first category, then add $(A,B)^2$ to S_2.

(ii). If link $(A,B)^1$ and $(B,A)^1$ are both in S_1, then we know that they both fall into the second category. Add either $(A,B)^2$ or $(B,A)^2$ to S_2 and the remaining one to S_3.

(iii). If link $(A,B)^1$ falls into the third category, and B is working in mode 3, then add $(A,B)^2$ to S_2. Otherwise if A is working in mode 3, add $(A,B)^2$ to S_3.

(iv). If link $(A,B)^2$ is in S_1, we know that it falls into the fourth category. Add $(A,B)^2$ to both S_2 and S_3.

It is clear, then, that $2\vec{R}(S_1) = \vec{R}(S_2) + \vec{R}(S_3)$, since for every $(A,B)^1 \in S_1$, $(A,B)^2$ is in either S_2 or S_3, and for every $(A,B)^2 \in S_1$, $(A,B)^2$ is in both S_2 and S_3. Next we need to show that $S_2, S_3 \in \mathbb{S}_{\text{MMa}}$. Assume to the contrary that $S_2 \notin \mathbb{S}_{\text{MMa}}$. This means that there exist two links $(A,B)^2$ and $(C,D)^2$ in S_2 such that C interferes with

B (more accurately, $\{C, B\} \in \mathcal{E}$), or $B = C$. However, if $B = C$, meaning that B is operating in full-duplex modes (mode 3 and 4) under schedule S_1, $(A, B)^2$ and $(C, D)^2$ cannot be both in S_2, according to the way S_2 and S_3 are constructed in the second and third category; if $\{C, B\} \in \mathcal{E}$, then we know that $(A, B)^x$ and $(C, D)^y$ cannot be scheduled simultaneously under FMa constraint set for any $x, y \in \{1, 2\}$. Thus, we have a contradiction, so $S_2 \in \mathbb{S}_{\text{MMa}}$. Similarly we can show that this is also true for S_3. ■

Note that in both the MMa/b and FMa/b constraint set, each node has two complete sets of RF chains, and both MIMO multiplexing modes and multi-user MIMO modes can fully exploit the potential of the two complete sets of RF chains. Then, one may reach the conjecture that part (d) and (e) in Equation (3) are actually equality signs, meaning that $\mathbb{D}_{\text{FMa}} = \mathbb{D}_{\text{MMb}} = \mathbb{D}_{\text{FMb}}$.

However, quite the contrary, Fig. 4 provides an **interesting counterexample** in which the throughput region achieved by the FMb constraint set is strictly larger than that achieved by MMb constraint set. This observation is somewhat surprising in that although Theorem 1 shows that the throughput region achieved by full-duplex communication is only a subset of that achieved by MIMO communication, when every node can choose to activate either MIMO communication or full-duplex communication, a larger throughput region may be achieved.

Also, Fig. 5 provides another simple counterexample in which the throughput region achieved by MIMO multiplexing is strictly a subset of that achieved by MMb constraint set, where every node can operate in either MIMO multiplexing, or multi-user MIMO modes.

Therefore, the next important question is, can we characterize all the network conditions under which we have $\mathbb{D}_{\text{FMa}} \subset \mathbb{D}_{\text{MMb}}$ and $\mathbb{D}_{\text{MMb}} \subset \mathbb{D}_{\text{FMb}}$. Theorem 2 and Theorem 3 below answer this question, where both necessary and sufficient conditions are given for the two strict inclusion relations to hold.

Theorem 2. *$\mathbb{D}_{MMa} \subset \mathbb{D}_{MMb}$ if and only if the network topology $\mathcal{G}$ contains a cycle with $2N_l$ nodes, where N_l is an odd number, such that if we label the nodes in that cycle sequentially from 0 to $2N_l - 1$, then there is no chord between a node with even label and a node with odd label.*

Proof: Before presenting the proof, let us first introduce some necessary notations.

For any $S_1 \in \mathbb{S}_{\text{FMb}}$, let $N_R(S_1) \triangleq \{A \in \mathcal{N} | A \text{ is receiving under schedule } S_1\}$. Then $N_R(S_1)$ is the set of nodes that operate in either mode 2, mode 3, mode 4, mode 6, mode 8, mode 9, or mode 10 under schedule S_1. Since FMb constraint set contains every possible modes a node can operate in, $N_R(S_1)$ is well-defined for S_1 being a feasible schedule under any other constraint sets.

For any $A, B \in N_R(S_1)$, we say A *affects* B under schedule S_1 when a flow received by node A is either transmitted by B or seen by node B as interference. Define

$$E_R(S_1) \triangleq \{\langle A, B\rangle | A, B \in N_R(S_1), \\ A \text{ affects } B \text{ under schedule } S_1\}.$$

Further denote the directed graph formed by $N_R(S_1)$ and $E_R(S_1)$ as $G_R(S_1) \triangleq \{N_R(S_1), E_R(S_1)\}$. Assume, without loss of generality, that there are M maximal weakly connected[1] subgraphs in $G_R(S_1)$. Denote the m^{th} such subgraph as $G_R(S_1^{(m)})$, where $S_1^{(m)}$ is the set of data links associated with the m^{th} subgraph, with $\cup_{m=1}^{M} S_1^{(m)} = S_1$. For any directed graph G, let $\widetilde{G}$ denote the corresponding undirected underlying graph.

Since each node in $N_R(S_1)$ is a receiver node, for any $A \in N_R(S_1)$, there is at most one node in $N_R(S_1)$ that affects A. Otherwise, if there are two different nodes that affect node A, then node A will see at least two interference flows and cannot be a receiver. This means, in the directed graph $G_R(S_1)$, the indegree of each node cannot be more than one.

The rest of the proof is done in the following two steps, where the details can be found in the technical report [13].

Step 1: we show that for any network topology $\mathcal{G} = \{\mathcal{N}, \mathcal{E}\}$, $\mathbb{D}_{\text{MMa}}(\mathcal{G}) \subset \mathbb{D}_{\text{MMb}}(\mathcal{G})$ **if and only if** there exists

[1]A directed graph is called weakly connected if replacing all of its directed edges with undirected edges produces a connected (undirected) graph.

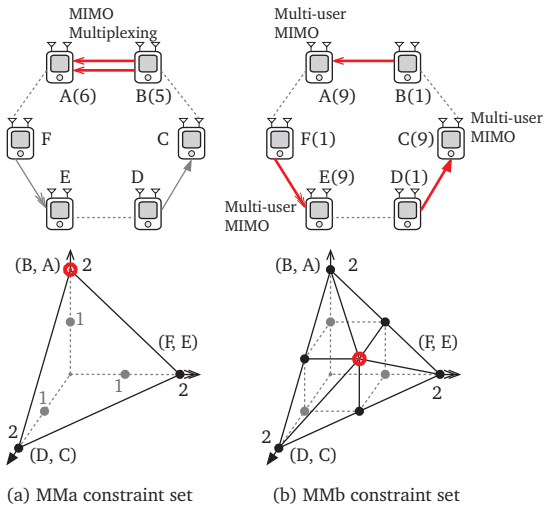

(a) MMa constraint set (b) MMb constraint set

Fig. 5. Throughput region of a six-node cyclic network under MMa/MMb constraint set. Here we only focus on three links: B to A, F to E, and D to C. Each dot in the throughput region plot represents a feasible schedule under the corresponding constraint set. The red arrows on each network graph illustrate one such feasible schedule, with the parentheses after each node represents its communication mode, and these feasible schedules correspond to the big red dots on the throughput region plot. (a) With only MIMO multiplexing enabled, no more than two data streams can be scheduled, but with multiuser MIMO capability at each node, three data streams, one for each link, can be activated simultaneously, as can be seen in (b).

$S_1 \in \mathbb{S}_{\text{MMb}}(\mathcal{G})$ such that $G_R(S_1)$ contains an odd length cycle.

Step 2: we show that for any network topology $\mathcal{G} = \{\mathcal{N}, \mathcal{E}\}$, there exists $S_1 \in \mathbb{S}_{\text{MMb}}(\mathcal{G})$, such that $G_R(S_1)$ contains a cycle with odd length N_l **if and only if** $\mathcal{G}$ contains a cycle with $2N_l$ nodes such that if we label the nodes on that cycle sequentially from 0 to $2N_l - 1$, then there is no chord between a node with even label and a node with odd label. ■

Theorem 3. *$\mathbb{D}_{MMb} \subset \mathbb{D}_{FMb}$ if and only if the network topology contains a cycle with $2N_l + N_f$ nodes, where $N_l + N_f$ is an odd number, and $0 < N_f < N_l$, such that we can divide the $2N_l + N_f$ nodes into two groups, group X with $2N_l$ nodes and group Y with N_f nodes that satisfy the following conditions: 1) If we label the nodes in group X sequentially from 0 to $2N_l - 1$, then there is no chord between a node with even label and a node with odd label. 2) The path on the cycle that connects any two nodes in group Y has even number of nodes in group X. 3) There is no chord connecting any node in group Y with the rest of nodes in the cycle.*

Proof: Similarly as that in the proof of Theorem 2, this proof comprises of the following two steps, where the details can be found in the technical report [13].

Step 1: we show that for any network topology $\mathcal{G} = \{\mathcal{N}, \mathcal{E}\}$, $\mathbb{D}_{\text{MMb}}(\mathcal{G}) \subset \mathbb{D}_{\text{FMb}}(\mathcal{G})$ **if and only if** there exists $S_1 \in \mathbb{S}_{\text{FMb}}$ such that $G_R(S_1)$ contains a cycle with odd length and at least one node in that cycle is operating in mode 3.

Step 2: we show that there exists $S_1 \in \mathbb{S}_{\text{FMb}}$ such that $G_R(S_1)$ contains a odd length with $N_l + N_f$ nodes, and $N_f > 0$ nodes in the cycle are operating in mode 3 **if and only if** $\mathcal{G}$ contains a cycle with $2N_l + N_f$ nodes, where $N_l + N_f$ is an odd number, and $N_f < N_l$, such that we can divide the $2N_l + N_f$ nodes into two groups, group X with $2N_l$ nodes and group Y with N_f nodes that satisfy the following conditions: 1) If we label the nodes in group X sequentially from 0 to $2N_l - 1$, then there is no chord between a node with even label and a node with odd label. 2) The path on the cycle that connects any two nodes in group Y has even number of nodes in group X. 3) There is no chord connecting any node in group Y with the rest of nodes in the cycle. ■

Corollary 3.1. *In a tree network topology, FMa/FMb constraint set and MMa/MMb constraint set lead to the same throughput region. In other words,*

$$\mathbb{D}_{MMa} = \mathbb{D}_{FMa} = \mathbb{D}_{MMb} = \mathbb{D}_{FMb},$$

when the network topology does not contain any cycle.

Remark 3.1. This Corollary follows directly from Theorem 2 and Theorem 3. The result implies that when the network topology formed by the interference relationship between wireless nodes does not contain any cycles, MIMO multiplexing alone can support the largest throughput region. In other words, neither multi-user MIMO nor full-duplex communication can provide any throughput gain when MIMO multiplexing is supported in every nodes.

Remark 3.2. It should be noted that Theorems 1-3 establish the complete characterization of the relationship between full duplex and MIMO, and provide us with a very clear guideline on which architectures and traffic patterns could result in improvement for one technology over another.

IV. Experimental Verification

In the previous sections, for analytical tractability, we focused on a binary interference model. This section presents results from an experimental testbed with software-defined radios for two purposes; (i) to verify if the throughput region claims are true in practice, and (ii) to present throughput comparison results as the SNR between nodes varies. Our results, indeed, corroborate the findings from the previous sections.

A. Experimental setting

1) **Setup***:* The nodes in our experiments are equipped with NI PXIe 1082 chassis [15] with two RF chains. Each RF chain consists of an XCVR 2450 (RF front end), an NI-5781 (data converter module) and an NI PXIe-7965R (Xilinx Virtex-5 FPGA). The nodes are capable of communicating at 2.4GHz wide-band. The supported carrier-level synchronization between RF chains from this platform helps with the MIMO and full-duplex implementation. We implement the OFDM transceivers for each RF chain. The communication system supports QPSK modulation with various coding rates (convolutional code 1/2, 2/3, 3/4).

The full-duplex implementation follows the design from [2], and the MIMO multiplexing implementation is based on the standard 802.11n protocol. For multi-user MIMO implementation, since the channel coefficient is not available at the transmitters, our system is effectively a multi-user MIMO system with the channel state information at the receiver (CSIR). Carrier-level synchronization is the only requirement in this case. LTE systems achieve this synchronization by having the receivers broadcast poll messages to which the transmitters synchronize [16]. However, this poll-based technique is not enough for our system since the synchronization has to be achieved across multiple collision domains. For instance, in the example shown in Fig. 4(f), nodes A and D need to be synchronized for the multi-user MIMO decoding at node E. At the same time, synchronization is also required for nodes B and D at receiver C. Thus, a receiver-initiated synchronization would result in a conflict at node D, which receives this poll from both E and C. To address this problem, one extra node in the experiment is assigned as reference node. It broadcasts, at a higher power, a known sequence as a reference signal. All the other nodes

adjust their frequency offset and starting time according to this broadcast signal. Note that there are many ways to achieve this synchronization, e.g., by using GPS signals or cellular control signals. Our goal is to compare different multi-RF chain configurations without introducing implementation specific biases.

2) **Environment***:* Our results are evaluated in an indoor environment. Specifically, the experiment is conducted inside our Computer Science department building, where there are multiple metallic cubicles. As the transmission is closely related to the conflict relationship of all the involved nodes, we use low transmission power (around -20dBm) and use walls made out of metal and bricks as blocks among nodes to create the desired interference map.

We operate at 2.437Ghz center frequency at night, as there is less interference. During the experiment, we find out that except for some periodical broadcast messages from cohabiting WiFi APs, nearly all of the interference signals are from within our experimental testbed.

3) **Method***:* To match the channel condition with available coding rates, we have a pre-calibration phase before the execution of experiment.

a) Initial Calibration: For each connected link in the network, we use the lowest available data rate (1/2 QPSK) under basic SISO transmission while keeping all the other links silent. We adjust the transmission power to the value where the packet reception ratio is just about to decline. The borderline transmission power is referred to as the *link's reference power*. Instead of choosing the optimal coding scheme for the observed SNR, this calibration allows us to pick the SNR for which the chosen coding scheme is optimal.

b) Execution: For each feasible schedule, we conduct our experiment under a set of 30 different channel conditions, where each channel condition is created by randomly and independently choosing a transmit power for each link with a value anywhere between its *reference power* and *reference power* + 10dB. For every link, each channel condition and each available channel coding rate, 100 packets are transmitted. For any specific link, the coding rate that maximizes the throughput will be adopted as the coding setting for the link. Following the above steps it can be guaranteed that the selected coding rate matches the channel condition.

4) **Metric***:* We omit carrier sensing and MAC overheads in the experiment as they are MAC protocol specific. All of the transmissions are unidirectional for a certain link. For each link, we define the link-rate under a certain schedule as the product of PER (packet error rate) and physical layer data-rate on that link, and the network throughput is defined as the sum of the long term average link throughput on each link.

B. Throughput result

We verify the throughput relationship between different constraint sets in a real experiment setup as described. Specifically, we build the network with topology shown in Fig. 4 here.

For every set of channel conditions, we conduct the experiment for four constraint sets: SS, FD, MMa, and FMb under two different scheduling configurations. The *two scheduling configurations* is shown in Fig. 6:

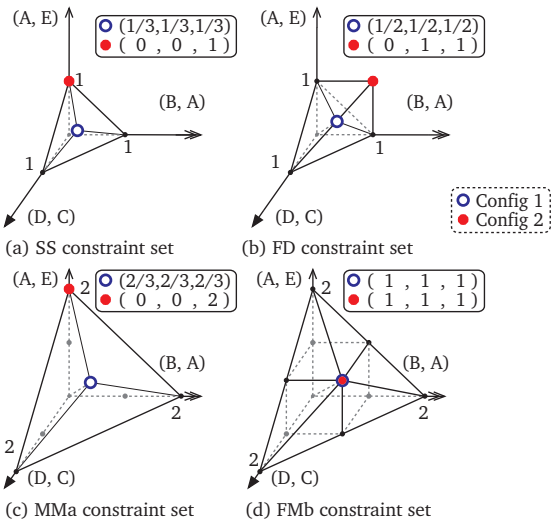

Fig. 6. Scheduling decision of two configurations for four different constraint sets: SS, FD, MMa, and FMb.

- *Config 1:* In this configuration, all the three links (D, C), (B, A) and (A, E) are guaranteed to transmit for the same amount of time.
- *Config 2:* In this configuration, we pick a fixed schedule for each constraint set, as indicated by the red solid dot in Fig. 6.

Figs. 7(a) and 7(b) present the CDFs of the network throughput with respect to the set of 30 different channel conditions under the two scheduling configurations, respectively. There are some points we want to highlight here:

- The full-duplex constraint set makes the major difference for the two figures. This is expected theoretically. As shown in Fig. 6, the average number of data streams of full-duplex constraint set is 1.5 for config 1 while the one for config 2 is 2.
- In both Figs. 7(a) and 7(b), the throughput relationship supports our theoretical result: The throughput of FMb is on average 27% higher than MMa constraint set while the theoretical result shows a 50% difference. This gap is mainly due to the residual signal after full-duplex cancellation and the inaccuracy of the synchronization regarding the multi-user MIMO communications. At the same time, note that when the SINR is high, the ratio of the throughput

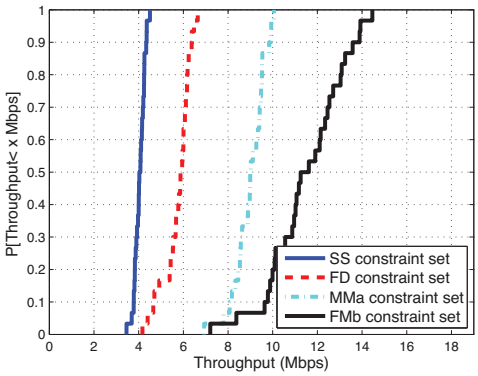

(a) CDF of throughput for config 1.

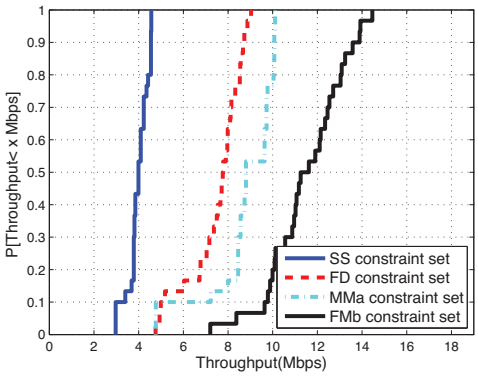

(b) CDF of throughput for config 2.

Fig. 7. CDFs of the network throughput w.r.t. 30 different channel conditions. (a) and (b) are the results corresponding to config 1 and 2 shown in Fig. 6, respectively.

between MMa and FMb is approaching 1.5, which is close to the theoretical result.

V. Conclusion

In this paper, we investigated the achievable throughput performance in wireless networks where each node can simultaneously activate two RF chains with no channel state information at the transmitter. There are three wireless technologies that can take advantage of the simultaneous activation of two RF chains, namely MIMO multiplexing, multi-user MIMO, and wireless full-duplex communication. We compared the throughput region achieved by some combinations of the three wireless technologies for a general network topology under a binary interference model. Our results provide a clear guideline on which architecture and traffic pattern could result in throughput improvement for one technology over another.

There are many interesting future directions that one can investigate: 1) Instead of considering the simplified throughput definition and the idealized binary interference model, we would like to extend the analysis to accommodate the more accurate SINR-based interference model. 2) Investigate the throughput performance in a general network where channel state information is provided at the transmitter. Here, a node in multi-user MIMO broadcasting can precode its two transmitted streams such that only one receive antenna (one active receive RF chain) is required at the two receivers each instead of two. 3) Generalize our results to the case when each node can have more than two active RF chains and different nodes potentially have different number of active RF-chains. 4) Instead of only focusing on the throughput region achieved by pure scheduling, i.e., interference avoidance, we would like to incorporate our analysis with more advanced physical layer technologies such as interference alignment [5] and cut-through transmission [4].

References

[1] D. Tse and P. Viswanath, *Fundamentals of wireless communication*. New York, NY, USA: Cambridge University Press, 2005.

[2] M. Jain, J. I. Choi, T. Kim, D. Bharadia, S. Seth, K. Srinivasan, P. Levis, S. Katti, and P. Sinha, "Practical, real-time, full duplex wireless," in *ACM MobiCom 2011*, New York, NY, USA, 2011, pp. 301–312.

[3] M. Duarte and A. Sabharwal, "Full-duplex wireless communications using off-the-shelf radios: Feasibility and first results," in *ASILOMAR 2010*, Nov., pp. 1558–1562.

[4] J. I. Choi, M. Jain, K. Srinivasan, P. Levis, and S. Katti, "Achieving single channel, full duplex wireless communication," in *ACM MobiCom 2010*, New York, NY, USA, 2010, pp. 1–12.

[5] V. Cadambe and S. Jafar, "Interference Alignment and Degrees of Freedom of the K-user Interference Channel," *Information Theory, IEEE Transactions on*, vol. 54, no. 8, pp. 3425–3441, 2008.

[6] S. Lim, Y.-H. Kim, A. El Gamal, and S.-Y. Chung, "Noisy Network Coding," *Information Theory, IEEE Transactions on*, vol. 57, no. 5, pp. 3132–3152, 2011.

[7] X. Lin, N. B. Shroff, and R. Srikant, "A Tutorial on Cross-layer Optimization in Wireless Networks," *Selected Areas in Communications, IEEE Journal on*, vol. 24, no. 8, pp. 1452 –1463, August 2006.

[8] M. Neely, E. Modiano, and C. ping Li, "Fairness and Optimal Stochastic Control for Heterogeneous Networks," *Networking, IEEE/ACM Transactions on*, vol. 16, no. 2, pp. 396 –409, April 2008.

[9] A. Eryilmaz and R. Srikant, "Fair Resource Allocation in Wireless Networks Using Queue-Length-Based Scheduling and Congestion Control," *Networking, IEEE/ACM Transactions on*, vol. 15, no. 6, pp. 1333 –1344, December 2007.

[10] A. L. Stolyar, "Maximizing queueing network utility subject to stability: Greedy primal-dual algorithm," *Queueing Systems*, vol. 50, no. 4, pp. 401–457, 2005.

[11] L. B. Le, E. Modiano, C. Joo, and N. B. Shroff, "Longest-queue-first scheduling under SINR interference model," in *ACM MobiHoc 2010*, New York, NY, USA, 2010, pp. 41–50.

[12] D. Qian, D. Zheng, J. Zhang, N. B. Shroff, and C. Joo, "Distributed CSMA algorithms for link scheduling in multihop MIMO networks under SINR model," *Networking, IEEE/ACM Transactions on*, vol. PP, no. 99, p. 1, 2012.

[13] Y. Yang, B. Chen, K. Srinivasan, and N. B. Shroff, "Characterizing the achievable throughput in wireless networks with two active RF chains," *Technical Report*. [Online]. Available: http://www2.ece.ohio-state.edu/∼yangy/

[14] C. Joo, X. Lin, and N. B. Shroff, "Understanding the Capacity Region of the Greedy Maximal Scheduling Algorithm in Multi-hop Wireless Networks," *Networking, IEEE/ACM Transactions on*, vol. 17, no. 4, pp. 1132 –1145, August 2009.

[15] "NI PXIe-1082 User Manual," Available at http://www.ni.com/pdf/manuals/372752b.pdf.

[16] "LTE version 11.3 Specifications," Available at http://www.3gpp.org/ftp/Specs/html-info/36331.htm.